Available online at www.sciencedirect.com

ScienceDirect

Advances in Space Research 55 (2015) 2438–2450

ADVANCES IN SPACE RESEARCH (a COSPAR publication)

www.elsevier.com/locate/asr

Simulated real-time lunar volatiles prospecting with a rover-borne neutron spectrometer

Richard C. Elphic [a,*], Jennifer L. Heldmann [a], Margarita M. Marinova [b,1], Anthony Colaprete [a], Erin L. Fritzler [c], Robert E. McMurray [c], Stephanie Morse [c], Ted L. Roush [a], Carol R. Stoker [a], Matthew C. Deans [d], Trey F. Smith [d]

[a] NASA Ames Research Center, Division of Space Sciences and Astrobiology, Moffett Field, CA 94035, USA
[b] Bay Area Environmental Research Institute, Space Science and Astrobiology Division, NASA Ames Research Center, Moffett Field, CA 94035, USA
[c] NASA Ames Research Center, Engineering Systems Division, Moffett Field, CA 94035, USA
[d] NASA Ames Research Center, Intelligent Systems Division, Moffett Field, CA 94035, USA

Received 6 October 2014; received in revised form 15 January 2015; accepted 21 January 2015
Available online 7 February 2015

Abstract

In situ resource utilization (ISRU) may one day enable long duration lunar missions. But the efficacy of such an approach greatly depends on (1) physical and chemical makeup of the resource, and (2) the logistical cost of exploiting the resource. Establishing these key strategic factors requires prospecting: the capability of locating and characterizing potential resources. There is already considerable evidence from orbital and impact missions that the lunar poles harbor plausibly rich reservoirs of volatiles. The next step is to land on the Moon and assess the nature, "ore-grade", and extractability of water ice and other materials. In support of this next step, a mission simulation was carried out on the island of Hawai'i in July of 2012. A robotic rover, provided by the Canadian Space Agency, carried several NASA ISRU-supporting instruments in a field test to address how such a mission might be carried out. This exercise was meant to test the ability to (a) locate and characterize volatiles, (b) acquire subsurface samples in a volatile-rich location, and (c) analyze the form and composition of the volatiles to determine their utility. This paper describes the successful demonstration of neutron spectroscopy as a prospecting and decision support system to locate and evaluate potential ISRU targets in the field exercise.
Published by Elsevier Ltd. on behalf of COSPAR.

Keywords: Moon; Volatiles; Rover; Neutron spectroscopy

1. Introduction

1.1. Lunar ISRU and a mission simulation

The Moon's polar regions clearly harbor a variety of volatiles. Several independent lines of evidence from Lunar Prospector (LP), the Lunar Reconnaissance Orbiter (LRO), and especially the Lunar CRater Observation and Sensing Satellite (LCROSS) impact mission point to the strong likelihood of cold trapped water ice and other species (cf. Feldman et al., 1998, 2000; Colaprete et al., 2010). Taken together, the evidence suggests that there are locations where water ice, at least, is present in sufficient abundance to warrant investigating its use for ISRU. There are extensive areas where surface and subsurface temperatures are sufficiently low to preserve water ice for over 1 Ga (Paige et al., 2010). However, not all these potential cold traps host similar abundances. Evidence of surface frosts is found in several permanently shadowed craters at the south pole, but not all (Gladstone et al., 2012). Some

* Corresponding author. Tel.: +1 650 604 4164; fax: +1 650 604 6779.
E-mail address: richard.c.elphic@nasa.gov (R.C. Elphic).
[1] Address: SpaceX, 1 Rocket Road, Hawthorne, CA 90250, USA.

http://dx.doi.org/10.1016/j.asr.2015.01.035
0273-1177/Published by Elsevier Ltd. on behalf of COSPAR.

but not all of these features have volumetrically significant hydrogen abundance (assumed to be in the form of water ice). Such a heterogeneous distribution of volatiles over hundreds of kilometers has been difficult to explain – why should equally effective cold traps not retain similar reservoirs of volatiles? Whatever the cause, such lateral heterogeneity may exist down to small scales, plausibly down to meters and tens of meters (Hurley et al., 2012).

Simply sampling in a cold, dark location at the Moon's poles does not assure finding significant, useful concentrations of volatiles. Surface mobility will be required to discover, map, characterize and in effect assay the "grade" of volatile deposits. Ease of extraction versus ore concentration and total volume is the trade. Therefore, a robotic mission to seek out and explore the volatile reservoirs of the Moon's polar region must be mobile and carry tools that permit the sensitive detection of surface frosts (in shadowed areas) and volumetrically significant bodies of hydrogenous materials.

As described by Sanders and Larson (2015) and Heldmann et al. (2015), the mission approach is unique and unlike rover operations on Mars, because operations are intended to be carried out in real time. This would be the case for a lunar polar rover mission with limited sunlight and power access. Based on current knowledge, the physical nature, distribution and chemical state of lunar polar volatiles at a given site are poorly known – in order to react to and capitalize on new discoveries and surprises, real-time operations must include mission operators, systems specialists and scientists. The decision as to when and where to interrupt a traverse for the risky, time-consuming and energetically expensive activity of sample acquisition and volatile processing involves more than engineering factors – real time data from the prospecting instruments are key. A major goal of the 2012 mission simulation included understanding what works, and what does not, in the area of supervised robotic prospecting and operations team decision-making.

Here we describe a field exercise in which the National Aeronautics and Space Administration (NASA) and the Canadian Space Agency (CSA) jointly developed, integrated and operated a lunar polar rover and prospecting/processing payload (see Sanders and Larson, 2015). This mission simulation had the goals of (1) locating near subsurface volatiles and assessing their ore quality in real time, (2) excavating and analyzing samples of volatile-bearing subsurface materials, (3) demonstrating the form, extractability and usefulness of the materials. The rover, provided by CSA, was the Artemis Jr. platform (for a description of the rover and its subsystems, as well as its performance in the 2012 exercise, see Cristello et al. (2013)). Instrumentation for prospecting and sample analysis was part of the Kennedy Space Center-managed integrated Regolith and Environment Science and Oxygen and Lunar Volatiles Extraction (RESOLVE) payload.

RESOLVE is a rover-based payload that includes several key instruments: (1) a neutron spectrometer subsystem (NSS) for assessing the volumetric abundance of hydrogen (including water) in the subsurface over which the rover is driving; (2) a near-infrared volatile spectrometer subsystem (NIRVSS) that senses surface hydration and mineralogy; (3) a drilling system (DESTIN, developed by NORCAT and provided by CSA) to auger and collect core samples down to one meter below the surface; (4) an Oxygen and Volatile Extraction Node (OVEN), that accepts samples from the drill system, seals and heats them, and conveys gaseous volatiles to (5) the Lunar Advanced Volatile Analysis (LAVA) subsystem, a gas chromatograph/mass spectrometer that analyzes water and other volatiles released from the heated samples. LAVA also incorporates a near-IR spectrometer in its surge tank (NIRST), which views the gaseous volatiles in the tank and provides additional assessment capability to the system.

As described by Heldmann et al. (2015), the primary prospecting instrumentation were the NIRVSS and NSS. Roush et al. (2015) describe the NIRVSS system, while the details of NSS can be found in Elphic et al. (2008). NIRVSS measures the reflectance spectrum over ~1.2–2.4 μm, from surface materials below the rover, as illuminated by a constant intensity lamp. NSS consists of two helium-3 gas proportional counter tubes that are sensitive to thermal and epithermal neutrons, the intensity of which correlates with bulk hydrogen in the soils. Both instruments were nearly collocated on the rover, and were run continuously while the rover was in operation. NIRVSS also included the Drill Operations Camera (DOC), which imaged the NIRVSS field-of-view and the auger and coring drill tools while in operation. In addition, forward-viewing navigation cameras returned imagery of the site, and a very wide-angle downward-viewing camera imaged the surface immediately below the rover.

The RESOLVE neutron spectrometer is similar to instruments flown on orbital missions including Lunar Prospector, Mars Odyssey, MESSENGER to Mercury, Dawn at Vesta, and aboard the Lunar Reconnaissance Orbiter (Feldman et al., 1999, 2002; Goldsten et al., 2007; Prettyman et al., 2011; Mitrofanov et al., 2010). A rover-borne neutron spectrometer can provide immediate measurements of the local hydrogen concentrations, allowing real-time monitoring and decision-making (Elphic et al., 2008). As the rover encounters volumetrically important hydrogen-bearing volatile deposits, NSS provides information that enables operators to halt the traverse and carry out more detailed characterization of the resource prospect. For this field test, the NSS resolution scale was a spot 25–30 cm in diameter, centered below the instrument.

The purpose of this paper is primarily to document the execution of the RESOLVE Hawai'i 2012 resource prospecting traverse plans, focusing on the NSS performance in detecting resource prospects and serving as a decision support tool. We also discuss the overall success of this prospecting approach with a view to how a similar technique may be used in a lunar polar rover mission to search for volatiles.

1.2. Field Test site and site preparation

The 2012 test site, located in Pu'u Haiwahine (19.7612°N, −155.4680°E), on Mauna Kea, had been used in previous testing of various parts of the evolving ISRU system. For the 2012 test, all instruments and payload subsystems were integrated with the rover. The rover was provided by Neptec under contract to CSA and was operated by members of the Neptec team in Hawai'i, as well as remotely from Canada. Communications, command and control of the rover and its payload were carried out from a remote mission operations center (MOC) at Hale Pohaku (19.7583°N, −155.4558°E), roughly 1.3 km to the east of the test site. The mission simulation was performed at 2470 m elevation. Additional support was provided by networked teams at NASA Ames Research Center, the CSA, and NASA Kennedy Space Center and Johnson Space Center. All operations were performed remotely from either the main MOC at Hale Pohaku, or by personnel at the control centers in the US mainland and the CSA's Exploration Development and Operations Centre (ExDOC).

The Pu'u Haiwahine test site is located between cinder cones in a valley. It contains pyroclastic materials derived from these cones, as well as windblown deposits from elsewhere on the volcano. The valley floor is largely composed of fine-grained soil particles, and contains relatively few clasts. The test site was cleared of vegetation to the maximum extent possible both to remove hazards to the rover and payload, and to make the site more Moon-like; vegetation might also produce unwanted effects in NSS. After arrival in Hawai'i, a subset of the team emplaced prospecting targets at specific locations in previously designed traverse plans. The test site and initial traverse plans are shown in Fig. 1. To avoid the difficulties of using water ice as prospecting targets (ice melts), buried high density polyethylene (HDPE) sheets were used as ice proxies. These proxies are squares of either 0.91 or 0.61 m on a side, and each was 1.25 cm in thickness. It was not possible to populate the entire test site with randomly distributed HDPE targets due to resource and time constraints, so they were placed at selected points along the pre-planned traverse paths and covered with a very thin layer of local soil (see Section 2.1); locations of the 15 emplaced targets were not known to the prospecting operations team. These targets would be "discovered" by the prospecting instruments, and real-time decisions would have to be made, whether to stop and investigate further, or continue along the planned traverse. Table 1 provides information on the 15 targets, including location and the number of each kind of HDPE sheets used, and whether or not the rover traverses actually crossed the targets.

In order to provide a way to core and retrieve samples of known hydration, and to compare the results from NSS with results from other instruments, a tube of prepared soil material (containing a controlled amount of water) was buried at each of the 15 target sites. For various reasons, including time and battery limitations during operations, not all targets were visited or drilled in the course of the test.

2. Field test operations

2.1. Traverse planning

Traverse planning was carried out prior to the test, and made use of pre-existing satellite imagery and topographic data, as described by Heldmann et al. (2015). The Exploration Ground Data System (xGDS) was used to plan rover traverses based on the perceived promise and geologic interest of features throughout Pu'u Haiwahine (cf. Fig. 7 in Heldmann et al., 2015). xGDS combines traverse planning and real-time telemetry display in a web-based application, and has been used in a large number of field exercises by various analog projects (Deans et al., 2013). Consequently xGDS had many mature capabilities suited to the Hawai'i field campaign. Traverse plans created in xGDS were exported to the RESOLVE operations system, translated, and from there were uploaded to the rover avionics system for execution. For this field exercise, we planned rover traverses based on visible albedo or color of surface materials seen in Google Earth satellite imagery, and topography. The intent was to cover a range of terrain features, and test the operability of the rover/payload system on various slopes and soil types. With xGDS, most relevant parameters are imported as layers so that traverse planners have access to each layer for the valley. Each layer can be switched on and off as visibility requires, giving the ability to quickly lay out or revise a traverse plan within operational areas and within hazard and slope limits, for example. The xGDS tools also permit estimation of durations for both individual transects and each traverse plan as a whole, so that planners can create plans that are suited to operational shifts of 8–10 h.

2.2. Description of the neutron spectrometer and pre-test calibration

At the Moon, Mercury, Mars and asteroids, galactic cosmic rays (GCRs) penetrate the surface and initiate nuclear reactions within the top few meters, resulting in neutron production. As mentioned in the introduction, these GCR-generated neutrons are the basis for orbital neutron measurements aboard several planetary missions. Thermal and epithermal neutrons can be very sensitive indicators of the presence of hydrogenous materials, so in a Moon, Mars or asteroid flight application, GCR-generated neutrons thus provide the neutrons needed for in situ prospecting. However, on Earth the atmosphere stops nearly all GCRs and prevents nearly all of them from reaching the surface; virtually no neutrons are created. In this case, one must rely on a radioactive neutron source to interrogate rocks and soils that the rover and instruments are traversing. The neutron source used for this test

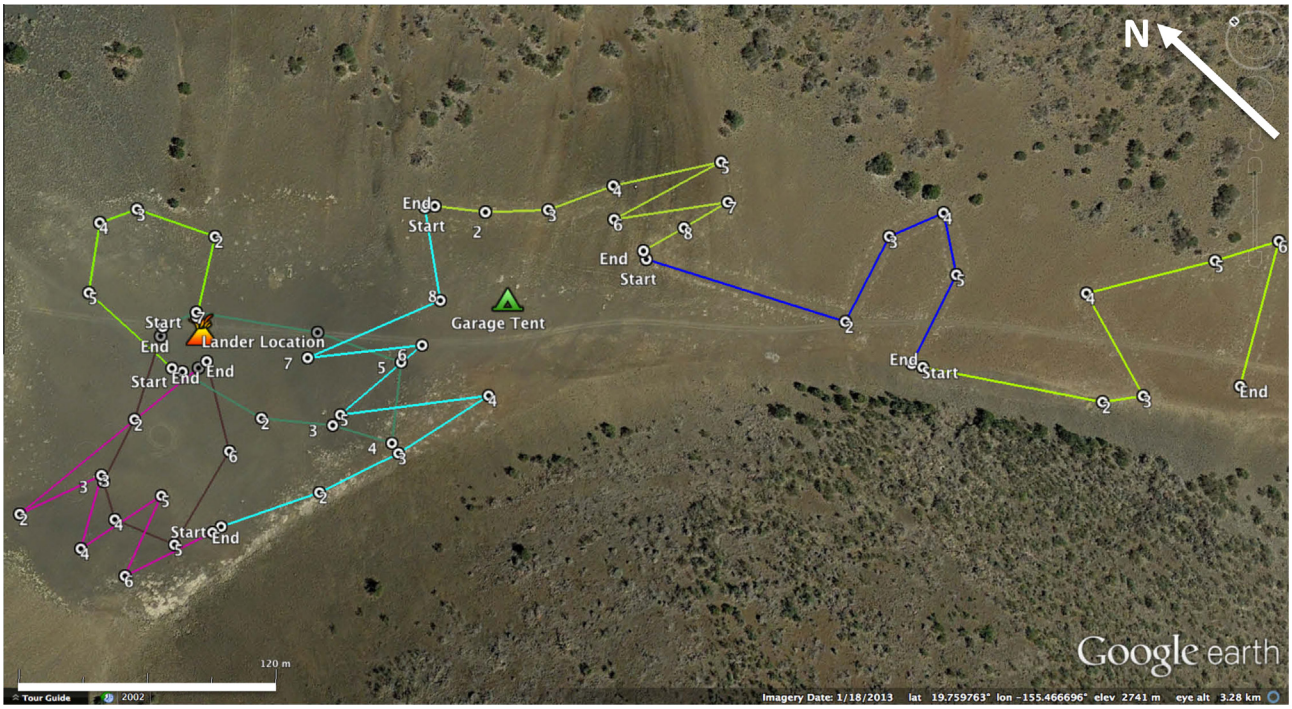

Fig. 1. The Pu'u Haiwahine valley, site of the 2012 field test. Shown here are the eight traverse plans developed prior to the test and designed to explore geologically interesting features in the valley. The scale bar at lower left is 120 m.

is a Frontier Technology Corporation Z100S sealed source, serial number FTC-CF-Z1154, with ~0.17 mCi activity (as of January 25, 2012). Because ^{252}Cf sources decay with time, we calibrated the neutron spectrometer immediately prior to field test operations, at ~04:30 UTC 13 July 2012, so that quantitative estimates could be made in real time during traverses.

The neutron spectrometer consists of two helium-3 gas proportional counter tubes. One detector admits all low-energy neutrons, whereas the other is covered by a thin layer of cadmium, which screens out the lowest energy (<0.5 eV) thermal neutrons. The detectors are very insensitive to the high energy (~2 MeV) neutrons coming out of the source. But when these fast neutrons interact with materials in the ground, they can be slowed (moderated) quickly if significant amounts of hydrogen are present. The greater the hydrogen abundance, the greater the moderating effect and the higher the returning flux of low-energy neutrons out of the soil materials. Consequently, the neutron spectrometer measures lower count rates when over hydrogen-poor materials and higher count rates when over wetter soils, ice or hydrous minerals.

Our calibration approach was to place HDPE targets of known thickness on a representative patch of Pu'u Haiwahine soil, and then drive the rover with payload across the targets. As shown in Fig. 2, the neutron spectrometer was mounted in a forward configuration and was operated with the same settings and thresholds that would be used in the traverse testing. The neutron spectrometer and source were located 15 cm above the local ground surface. The calibration targets were 1.25, 2.54, 3.81, and 5.08 cm thick high-density HDPE squares. HDPE has a density slightly greater than water ice, 0.95 versus 0.915 g/cm^3, and like water has a very high hydrogen concentration. The relevant physical parameter for neutron moderation in materials is the product of the average fractional energy loss per elastic-scattering collision and the macroscopic cross section for elastic scattering, $\xi_s\Sigma s$, which depends on material composition (Feldman et al., 2000). The quantity $\xi_s\Sigma s$ is 1.36 for pure H_2O, but is 1.76 for high-density polyethylene (units are cm^2/g). In other words, a centimeter of high-density polyethylene has the effective energy-scattering properties of 1.76/1.36 = ~1.3 cm of water ice. For this reason, the targets above correspond to ice column densities of ~1.5, 3.1, 4.7 and 6.2 g/cm^2. For comparison, a soil of non-hydrous mineralogy with a mass density of 1.5 g/cm^3 and 5-wt% moisture content has 1.5 g/cm^2 of H_2O if integrated over the top 20 cm (about 6 neutron scattering lengths). For our calibration test, the rover speed was ~10 cm/s for the first set (hr 4.5–4.6), and 20 cm/s for the second pass done in reverse. The slower pass provided better target spatial resolution and statistics.

Fig. 3 shows the clear rise in thermal count rate with target thickness, expressed as equivalent excess H_2O-equivalent column density (g/cm^2). We use the term "excess" to emphasize the fact that the Pu'u Haiwahine valley soils have a variable but non-negligible level of moisture (~1–10 wt%), and that the prospecting targets represent a significant increment of equivalent-hydration above this background level. This calibration curve allows us to convert the measured NSS thermal count rates observed throughout the test to equivalent ice column densities, an

Table 1
Scorecard for in situ resource prospecting.

Target #	Max HDPE layers	GPS position: latitude, longitude	HDPE excess H_2O (g/cm^2)	NSS estimated excess H_2O (g/cm^2)	Comment
Target 1	1	19.761837°, −155.467884°	1.5	2.1	Detected and mapped: Phase1_PlanA_v5 (7–14/22:37UTC)
Target 2	2	19.761464, −155.468215	3.1	3.3	Detected and mapped: Phase1_PlanA_v5 (7–15/01:40UTC)
Target 3	1	19.760795, −155.468112	1.5	—	Missed: Phase2_PlanF_v1 due to going off plan, plus telemetry drop
Target 4	3	19.760608, −155.46754	4.7	3.9	Detected and mapped: Phase2_PlanF_v1 (7–16/22:11UTC)
Target 5	1	19.761272, −155.468396	1.5	—	Originally on Phase1_PlanC_v5, but not on Phase2_PlanA_v6 traverse path
Target 6	2	19.761183°, −155.468842	3.1	3.9	Initially missed due to ExDOC driving far off plan: Phase2_PlanA_v5. Detected/mapped after rover directed back on path
Target 7	1	19.760572°, −155.467746°	1.5	—	Not visited due to revised execution of Phase2_PlanB_v5.
Target 8	2	19.760733°, −155.467055°	3.1	2.0	Detected but not mapped on Phase2_PlanB_v5, due to slope concerns (7–17/00:19UTC)
Target 9	1	19.760291°, −155.466158	1.5	1.5	Detected and mapped: Phase2_PlanC_v7, AIM difficult due to slope (07–17/02:00UTC)
Target 10	3	19.760018°, −155.466348	4.7	3.7	Detected but not mapped on Phase2_PlanD_v7, AIM waived (7–17/19:50UTC)
Target 11	3	19.759619°, −155.46616	4.7	3.7	Detected and mapped: Phase2_PlanD_v8 (07–17/20:21UTC)
Target 12	2	19.759287°, −155.465748	3.1	—	Not visited due to revised plan: Phase2_PlanD_v8 (07–17/20:21UTC)
Target 13	1	19.758932, −155.465842°	1.5	2.0	Detected but not mapped on Phase2_PlanD_v8, AIM waived due to "not very hot" (7–17/22:12UTC)
Target 14	2	19.758249°, −155.465485°	3.1	3.0	Detected and mapped: Phase2_PlanE_v6 (07–17/22:55UTC)
Target 15	3	19.758141°, −155.464356°	4.7	—	Not visited due to truncation of plan Phase2_PlanE_v6

important capability in decision support of resource prospecting and characterization.

2.3. Prospecting decision thresholds

For the purposes of this test, a sustained increase in the NSS thermal neutron count rate above 50 count/s for more than 10 s, was considered to be an actionable trigger point for tactical decision making. This value was chosen because it is over 3 standard deviations above the typical valley soils value of ~30 counts/s. Crossing this threshold indicates that the rover had come across an area of significantly enhanced hydrogen (water) concentration, meriting further investigation and decision-making. Operationally, crossing this threshold could transition the mission from *Prospecting* mode to a mode in which the potential resource itself is mapped at finer scales, referred to as "*Area of Interest Mapping,*" or *AIM* (see Heldmann et al., 2015). In *Prospecting* mode, the rover follows the pre-planned traverse, hazards permitting, with the spectrometers mapping hydration and mineralogy as the rover moves across an area. But upon crossing this pre-determined threshold, the mission operators would issue a real time command to halt. Using the data from the prospecting instruments, the science and mission operations team then decides whether to transition to the *AIM* mode. For various reasons they may choose to forego the time and energy required to map out the potential resource body, and instead carry on with the remaining prospecting traverse. But if the feature is deemed interesting, the rover then executes a pre-planned *AIM* to assess the size and abundance of the potential resource.

As described in Heldmann et al. (2015), if the *AIM* reveals a suitable prospect, the mission then transitions to a subsurface assessment mode. This mode entails the drill augering into the prospect while NIRVSS views the cuttings that are brought to the surface. If evidence of hydration is seen in the near-IR spectrum, the operations team may elect to core the prospect, acquiring a sample for analysis by OVEN and LAVA.

2.4. Test execution

Here we describe some of the key results of the prospecting and characterization activities during the 5 days of the field test. The first day is discussed in some detail in order

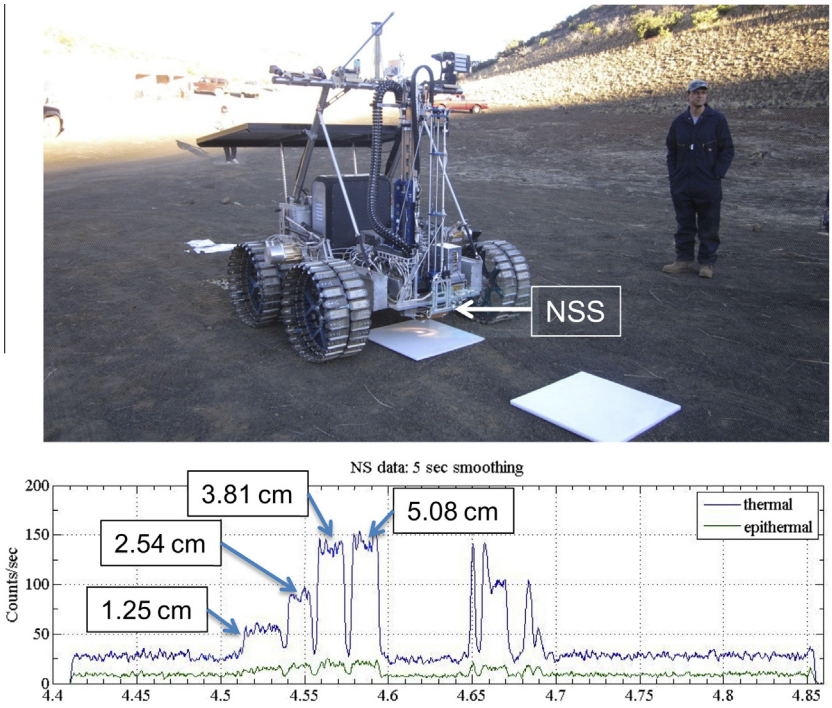

Fig. 2. (Top) high-density polyethylene (HDPE, an ice proxy) calibration targets for the neutron spectrometer subsystem (NSS). (Bottom) neutron spectrometer calibration data. The enhancements in count rates correspond to 1.25, 2.54, 3.81, and 5.08 cm thickness HDPE targets, respectively. This is equivalent to ~1.5, 3.1, 4.7 and 6.2 g/cm^2 column density of water ice. Rover speed was ~10 cm/s for the first set (hr 4.5–4.6), and 20 cm/s for the second set (hr 4.65–4.7).

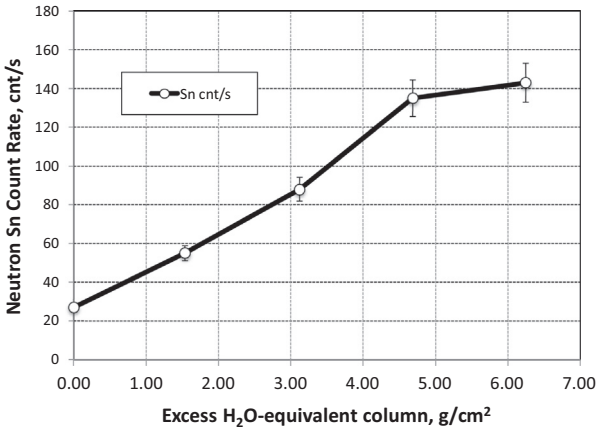

Fig. 3. Calibration curve for thermal neutron count rates against excess H_2O-equivalent column abundance, expressed in g/cm^2. These values are in excess of the moisture or mineral hydration already in the site soil.

to acquaint the reader with some of the prospecting procedures and activities. Thereafter we move quickly through the following days.

2.4.1. Initial exploration following lander egress and checkout

On 14 July 2012, the initial operational traverse plan was executed (the green plan at left in Fig. 1). It was designed to simulate the initial limited exploration of an area to the northeast of the lander, following egress from the lander and successful rover/payload checkout. The total traverse distance was intentionally short, only ~50 m, being both a conservative test of the rover and payload ability to execute the plan and return real time data. Fig. 4 shows a map of this plan as executed. The color-coded path is NSS thermal neutron count rate, laid down on the base map satellite image of the area. The rover path never deviated more than 2 m from the planned traverse. The background count rate for soils in this area is ~30 count/s, but large increases were seen at two locations, referred to hereafter as "hotspots", denoted by (A) and (B). The operations team discovered Target 01 at hotspot A (Fig. 4). (Recall that the team had no knowledge of where the buried target was, so the transition of the neutron spectrometer data across the 50 counts/s threshold was not expected.) Upon crossing the threshold, an "all-stop" was called, halting the rover's progress. At this point, the operations team elected to transition from *prospecting mode* to *AIM* mode, defining the extent and potential of the feature.

The *AIM* pattern was developed to provide good coverage at meter scales in the least amount of time spent in execution. As can be seen in Fig. 4, upper right, execution of the pre-planned, block-spiral *AIM* traverse pattern resulted in gaps of coverage, owing to the realities of rover slip on hillsides, and other traverse issues. While the idealized pattern, shown at lower right of Fig. 4, would have provided good coverage, it was difficult to accomplish without coverage issues. The subsequent *AIMs* in this field test permitted more interactive driving, in order to fully exploit the situational knowledge available to both the

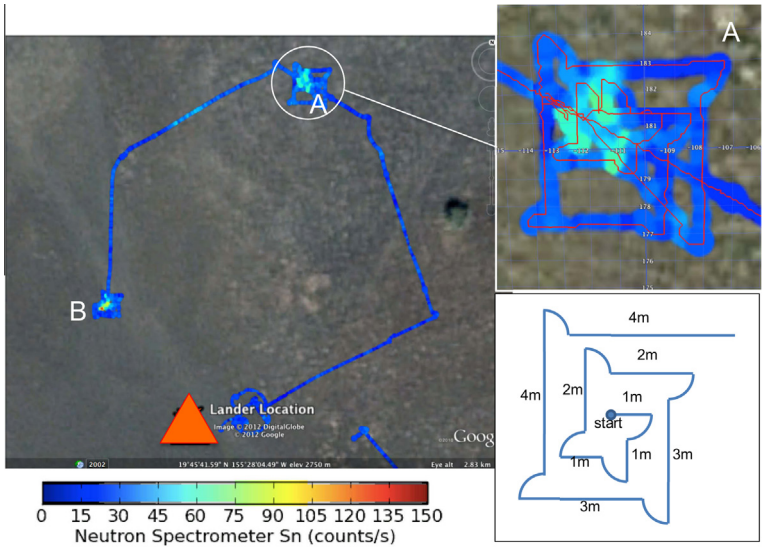

Fig. 4. (Left) the first traverse, executed on 14/15 July, 2012 UTC, with NSS thermal neutron count rates overlaid. Two detected hydrogen hotspots, A and B, are also shown. (Upper right) the first area of interest mapping (*AIM*) left gaps due to rover slip and traverse issues. It was difficult to execute the pre-planned *AIM* pattern (lower right) without leaving gaps.

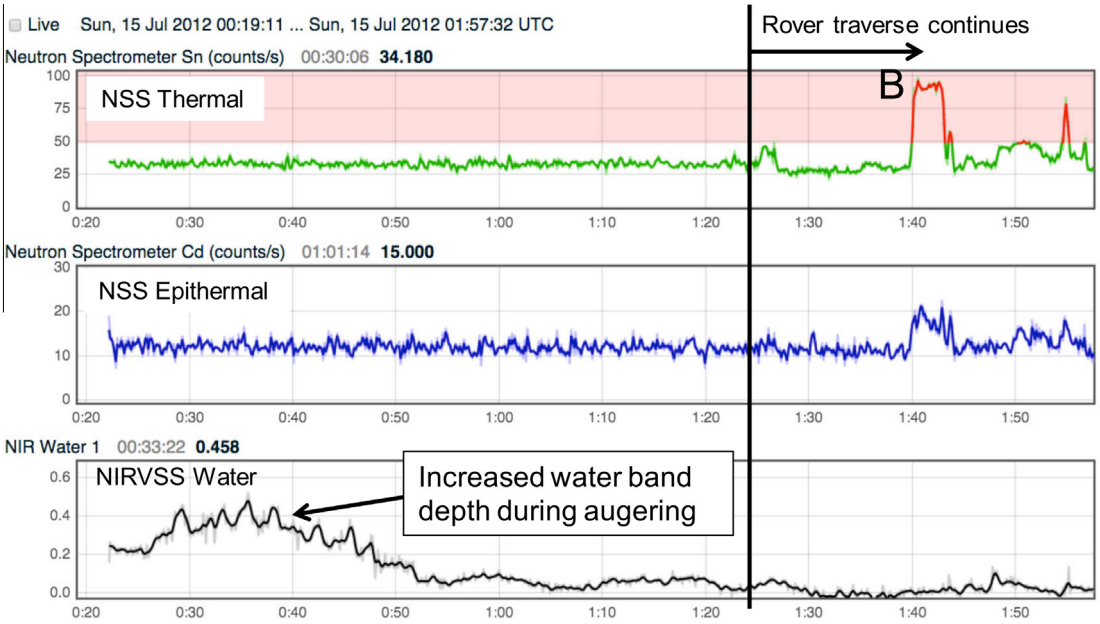

Fig. 5. Strip chart plots of NS thermal (top), epithermal (middle) and NIR water band depth 1 (bottom) for 15 July 2012/00:19–01:57 UTC. Note trigger threshold of 50 counts/s in the thermal (Sn) channel. Increased moisture was observed by NIRVSS during augering. Hotspot B (Target 02) at was detected at 01:40 UTC.

rover driver and the scientists. The direct interaction of rover navigation with science displays and guidance resulted in much more complete coverage of prospective resource targets.

It was decided to auger at the hotspot, and NIRVSS observations of the cuttings indicated higher hydration in the subsurface. This can be seen in Fig. 5, which shows an example of an xGDS time-series strip chart used for real time decision-making. Here NSS thermal and epithermal count rates as well as a NIRVSS water band parameter (band depth of H_2O absorption at 1.5 μm) are plotted for 2012–07-15/00:19 – 01:57, which encompasses the auger activity at hotspot A, and shows the discovery of hotspot B. NIRVSS measured increased band depth during augering from 00:19 to 00:50 UTC, indicating that cuttings brought up by the auger had greater moisture content. Following rover traverse restart at 01:22, the 50-count/s threshold was crossed at hotspot B. The subsequent *AIM* activity made use of interactive guidance provided by the real time science console to cover the hotspot.

Count rates at hotspot B (Target 02) rose even higher than in hotspot A (Target 01). This find also prompted a

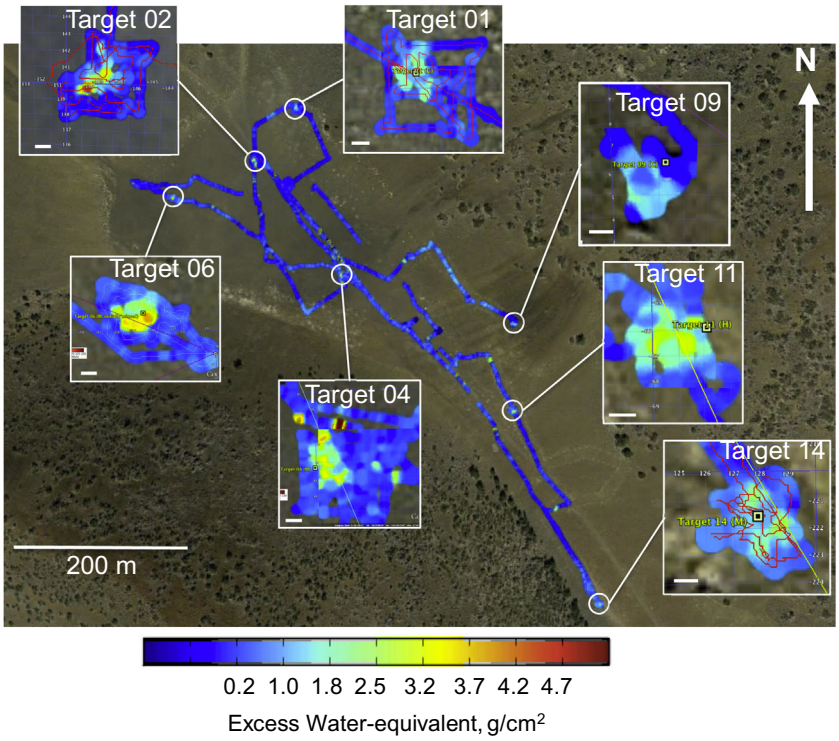

Fig. 6. Neutron spectrometer tracks for all traverses executed in the test, with insets for the seven *AIM*s. White scale bar in the insets denotes 1 meter.

transition to *AIM*. During the *AIM*, an especially high thermal neutron count rate was observed over a small area. This feature was identified as a location at which augering and evaluation of subsurface cuttings would also be carried out. The results were promising, and coring would be planned for and samples acquired for analysis by the OVEN and LAVA on the next operational shift.

2.4.2. Prospecting and area of interest mapping

Fig. 6 captures the entire Prospecting and *AIM* execution of the field test, from 14 to 19 July, 2012. Insets illustrate the detailed features for each target for which an *AIM* was executed. The hotspot features as measured will be discussed and then compared to after-test information about each target.

2.4.3. Day 1, 14 July 2012: AIM results

The traverse details for 14 July have already been discussed. Here we describe the potential resources that *AIM*s revealed during the traverse. As seen in Fig. 4, Hotspot A (Target 01) shows three distinct elongate highs in count rate, each less than 1 m wide but over 1 m in length, spanning an area of several meters in extent. The local highs of roughly 60–70 counts/s in thermal neutrons would correspond to 1.5–2.0 g/cm^2 of water ice column density. Hotspot B (Target 02) also has several local maxima, each of 1-meter scale. There is also a small area of very high flux, >120 counts/s that would correspond to an excess water ice column density of >4.2 g/cm^2. This feature was identified as a location at which augering and evaluation of subsurface cuttings would be desired.

2.4.4. Day 2, 15 July 2012: location of potential resource and subsurface sample acquisition

On July 15, 2012, the Artemis Jr rover was re-located to the previous day's hotspot B (Target 02), where it would drill and core sample. Because of offsets discovered in GPS positions, the neutron spectrometer was again put to use to perform *AIM*. Once the desired feature was re-located, augering proceeded. Roush et al. (2015) discuss the details of augering and the mineral forms identified by NIRVSS during this activity. With promising identification of hydration by NIRVSS, there followed coring and retrieval of the sample for processing. In the end, between 80 and 95 cm of core was obtained. The core sample was then analyzed in OVEN and LAVA operations.

2.4.5. Day 3, 16 July 2012: prospecting plan and auger operations

On July 16, 2012, the traverse plan took the rover/payload across new territory SE of the landing site. The rover encountered Target 04 around 21:47 UTC, shown by the inset in Fig. 6. Count rates above 100 counts/s pointed to a significant hydrogen abundance, and elevated levels were observed over an area several meters in extent.

After the *AIM* activity revealed an especially enhanced signal at this site, it was decided to proceed with auger mode. Excavation commenced at 22:45 UTC and subsurface material was monitored by the NIRVSS spectrometer.

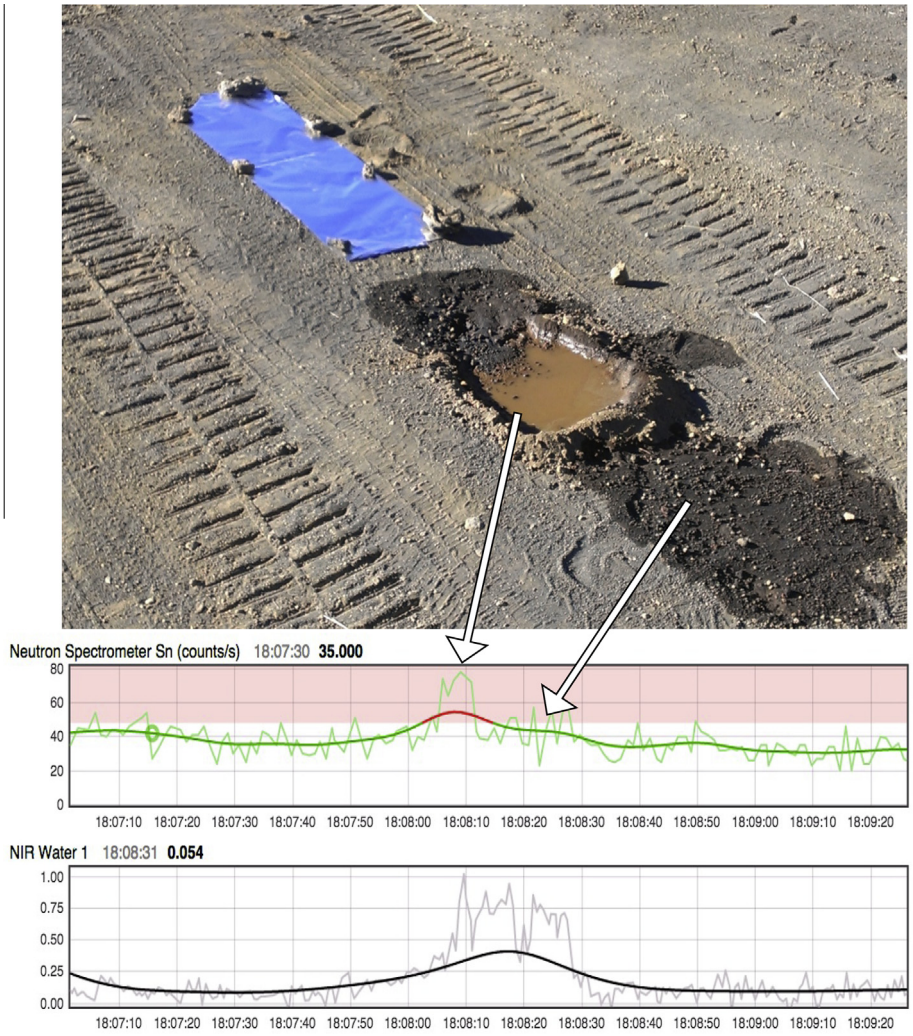

Fig. 7. (Top) short traverse over aluminum foil and liquid water. (Bottom) NSS and NIRVSS signatures of the water puddle. Note the unsmoothed NSS data suggest column abundance of ~2.5 g/cm^2. The damp area has lower abundance, consistent with 1 g/cm^2, still higher than the background of unmoistened soil.

Evaluation of the auger activity led the team to forego coring at this site; the traverse picked up again and the rover proceeded to the next waypoint, roughly 19 m to the north.

At 2012-07-17/00:16:00 UTC, the neutron spectrometer count rate threshold was again crossed, "All Stop" was called, and the operations team evaluated the signal. The thermal neutron count rate had climbed from a background of about 30 to 65 count/s, corresponding to roughly 1.5 g/cm^2 column abundance of water-equivalent hydrogen. An *AIM* was waived, for two reasons: (1) the area had a significant slope that would make executing the mapping pattern difficult, and (2) the feature was judged not sufficiently rich to justify the time out of the roving plan. The time from threshold crossing to decision was roughly 5 min. This hotspot was Target 08 (see Table 1).

The next traverse plan took the rover to the SE along the slopes of the NE edge of the valley. Neutron spectrometer readings flirted with the 50 count/s threshold, but were never sustained enough (10 s continuous or more) to call an "All Stop". Due to the difficult slope, the rover was manually driven to the waypoints of the plan rather than teleoperated. About 11 m beyond waypoint 4, NSS crossed a threshold for an "All Stop" and assessment. The resulting *AIM* activity is shown in the inset for Target 09 in Fig. 6. This feature appeared to be a ring-like structure with a central minimum in water-equivalent hydrogen abundance. The maximum ice column density seen corresponds to 1.5 g/cm^2. The team elected to core this location in order to have a sample for OVEN and LAVA to analyze overnight.

2.4.6. Day 4, 17 July 2012: prospecting plan and auger/coring operations

On July 17, 2012, the traverse plan continued SE of the previous day's area. By 19:46 UTC the rover was at the starting point, and by 19:48 we had already encountered a neutron hotspot, just 3 m from the initial waypoint. "All Stop" was called, but after deliberating, the team elected to press on to the next waypoint. This hotspot, Target 10, was

consistent with 1.5–3.1 g/cm^2 of water ice, the most intense area being about 1 m in extent along the traverse path.

At about 20:08 UTC, the rover encountered another hotspot, this time with rates approaching 90 counts/s; this was Target 11. After an "All Stop" the team elected to do an *AIM* activity, as shown in Fig. 6, inset Target 11. Upon completion of the *AIM* procedure, the feature was seen to consist of 3 separate hotspots, between 0.5 and 1 m in size and separated by 1–2 m. Each hotspot was consistent with 3.1 g/cm^2, and surrounded by a background of 1.5 g/cm^2 water-equivalent material. The overall feature size was roughly 3 m × 2.5 m. The team chose to move into auger mode, and the rover was positioned to execute this. The resulting cuttings pile was small, presumably because the augering process simply compacted the material in the prepared sample tube. The team chose not to collect a core because little evidence of moisture was seen.

At 21:33 UTC, a new plan was begun and by 22:10 the NSS data passed threshold again; an "All Stop" was called. This was Target 13, but an *AIM* procedure was waived because the feature was only showing 1.5 g/cm^2 of ice equivalent, and the terrain was vegetated and likely to cause rover hazard avoidance issues. The final waypoint for the traverse plan was 8 m beyond the hotspot.

The next traverse plan was initiated at 22:22 UTC, and took the rover still further to the SE. ExDOC at CSA was controlling the rover at this time, and performed some hazard avoidance maneuvers that took the robot off the traverse path. However, after working to get back on the plan, the rover crossed the 50 counts/s threshold at 22:43 UTC. Target 14 (Fig. 6) had been located. The onsite operations team elected to perform *AIM*, working with ExDOC at CSA to perform the activity. Once again, there appeared to be three separate hotspots, each slightly less than 1 m in size, spread over an area roughly 3 m in N–S extent, by 2 m in E–W extent. The peak neutron signature suggests an abundance of ~3.1 g/cm^2. The team elected to auger at this site, and then to core in the tube of prepared soil. This coring activity completed the operational day, and the rover returned to base at 18 July/03:00 UTC.

2.4.7. Day 5, 18 July 2012: OVEN/LAVA sample processing day

18 July 2012 was committed to working technical issues and troubleshooting the OVEN and LAVA operations. No prospecting operations were carried out.

2.4.8. Day 6, 19 July 2012: public affairs/outreach and roving operations

A demonstration of the rover prospecting operations for film crews was scheduled for this day. Traverse operations would be truncated, covering a shorter period of time than previous day's activities. However, two activities would prove useful for both NIRVSS and NSS: (1) driving over a prepared puddle of water and (2) rover ingress and egress from the lander. The former provided data for both NIRVSS and NSS while actually traversing a thin layer of liquid water, and the latter would provide information to NSS about signal from the soil versus background from the rover. Then the rover would egress the lander, mimicking flight, and proceed to a prospecting traverse plan.

Fig. 7 shows the traverse across the thin aluminum foil and liquid water targets. NSS and NIRVSS signatures of the water puddle are shown in the lower panel. Note the unsmoothed NSS data suggest a water column density of ~2.5 g/cm^2. The small (~20 cm) damp area to the lower right has lower water apparent water abundance. It was insufficient to trigger the 50 counts/s threshold, but higher than the background of nearby soil. NIRVSS measurements clearly show comparable band depths for both the puddle and the moistened area (the offset in time between NSS and NIRVSS corresponds to the difference in their respective fields of view of approximately 50 cm).

As the rover climbed the lander ramps, the distance between the NSS and the ground increased, and the thermal neutron return from the ground decreased. The reverse occurred as the rover egressed the lander. Fig. 8 shows the rover atop the lander, and the NSS record of egress down the ramps onto the local surface between 19:40 and 19:50 UTC on 19 July 2014. At normal operating height (15 cm off surface), the count rate was 25–30 counts/s, whereas near the top of the ramp it was ~7–8 counts/s. This low and constant background count rate is present in all the traverse data.

The next traverse plan was initiated at 2012-07-19/20:22 UTC; this plan would take the rover to an unsampled area W of the landing site. ExDOC was in control of the rover. The traverse soon deviated from the planned transect, due to rock avoidance around 20:30 UTC. At 20:36 UTC, 11 m north of the planned traverse, the rover was re-steered back on plan, and successfully attained waypoint 2. Thereafter, however, deviations began again.

A halt was called at waypoint 3 of the traverse plan (not shown). The rover was driven back along the planned traverse path, where Target 06 was discovered, and "All Stop" was called. The strength of the signature, seen in Target 06 of Fig. 6, pointed to a column density of ~3.8 g/cm^2 of ice-equivalent column abundance, so the team decided to transition to *AIM*. The *AIM* process went from 21:15 to 21:23 UTC, or about 8 min, demonstrating that a direct coordination between console positions is highly effective. This feature evidenced more structure than other hotspots, with a localized peak having dimensions of ~0.5 m by ~0.5 m, and extended areas of elevated hydration up to 2 m W of this peak. Also seen was an isolated high 2 m W and slightly N of the peak, as well as an extended local hydrogen increase just N and a little W of the main peak.

2.5. Post-test target comparison with test data

The Hawai'i team members who had emplaced the HDPE targets provided the locations and target thicknesses in Table 1 after the test. We compared those numbers to

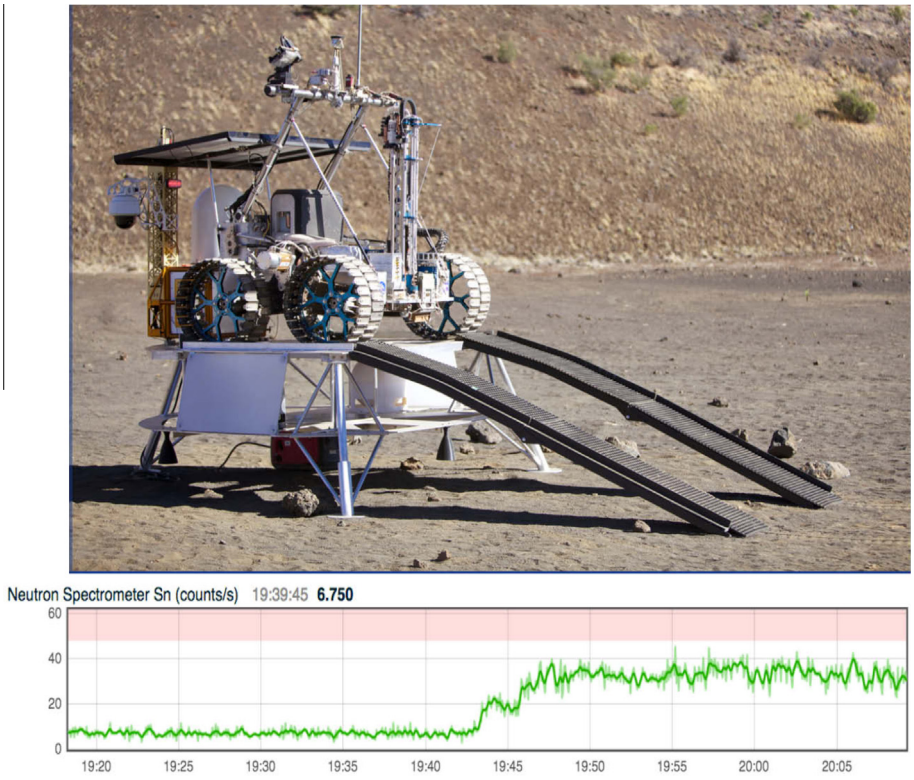

Fig. 8. (Top) Artemis Jr rover atop the field test lander. (Bottom) NSS thermal neutron signature of egress, showing the rise in count rate as the source and detectors approach the ground. This is a valuable exercise for estimating background due to rover materials.

the measured maximum count rates recorded by NSS at each feature. Fig. 9 shows the comparison of the maximum estimated excess water-equivalent column versus the maximum thickness of HDPE layers used to make the targets. Also shown on the upper scale is the HDPE water-equivalent excess column density. The correspondence clearly shows that NSS can gauge this quantity consistently. Some of the variability in detected signal is related to the variable depth of soil cover used to "hide" the HDPE targets (these were hidden to mimic subsurface deposits and to avoid giving visual clues to the operations team). When the targets were removed, it was noted that the soil immediately beneath was damp, more so than surrounding soils at the same depth, and water had collected on the bottom of the HDPE. Apparently water vapor from wetter soil layers at greater depth diffused upward and condensed on the bottom of the impermeable HDPE targets. For thin, one-layer targets, this additional moisture evidently added a detectable increase in HDPE hydrogen signal and produced a slight elevation of thermal neutron return. This explains why the apparent excess ice column density is actually higher than would be expected for a one-layer HDPE target in Fig. 9. Such a moisture layer adds little to the thicker stacks of HDPE.

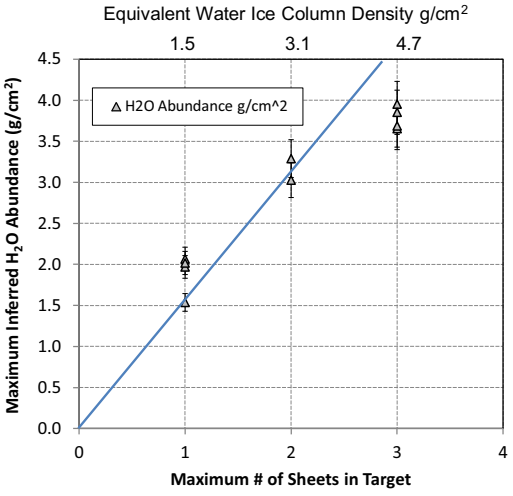

Fig. 9. Measured neutron spectrometer maximum excess H_2O abundance for the ten detected targets, versus the maximum thickness of polyethylene sheets emplaced by the out-of-simulation team members.

3. Lessons learned: prospecting operations in real time

Several aspects of the Hawai'i 2012 test taught the RESOLVE team valuable lessons that may be applicable for a flight mission. Three are below.

3.1. AIM procedure issues

3.1.1. Issue/observation

Executing the *AIM* procedure as originally designed resulted in gaps in coverage by NSS and NIRVSS. These gaps resulted from the realities of rover operations on real terrain, where slope slip and other difficulties skew the

actual traverse. For this reason, incomplete coverage of the area led to missing a suitable hotspot. The field test was the very first opportunity to use this procedure under realistic circumstances; it had not been previously tested.

3.1.2. Resolution

Rover and science operators quickly understood the difficulties. Instead of blindly executing a pattern without guidance from real time data, a more adaptive approach was adopted. Rover navigation and science worked closely together, viewing the same instrument map displays in xGDS, to proactively fill in gaps and more thoroughly cover the hotspot area. More efficient characterization of potential resource abundance and distribution was achieved.

3.1.3. Recommendation

Further development of the rover navigation/real time science partnership should be explored, since the most efficient method of homing in on a desirable hotspot was when a well-informed rover driver directed the robot to quickly fill in gaps. Situational awareness tools must include relevant instrument data displays, such as the xGDS raster maps shown in this paper.

3.2. Rover navigation from remote control centers

3.2.1. Issue/observation

Rover navigation from the Hale Pohaku control center used an up-to-date version of xGDS to provide guidance and situational awareness with respect to the two prospecting instruments, NSS and NIRVSS. However, when the rover was being driven by controllers at a remote center (ExDOC), the operators there did not initially have the xGDS website up and running. This hampered their ability to effectively carry out traverse and *AIM* procedures.

3.2.2. Resolution

At times it was necessary to return control to Hale Pohaku in order to stay on the plan and the timeline. These handovers consumed operations time but did result in coverage of desired regions of interest.

3.2.3. Recommendation

In a large, highly distributed team, it is vital to designate a testing lead who works across organizational lines to ensure that all detailed procedures and technical systems are integrated well in advance, and operationally tested before the field activity. In the future, software like xGDS should be in test-ready form, and all relevant operations entities should be trained on and familiar with its use in that form. Realistic training with relevant software and website tools is critical to executing traverses and *AIM* procedures efficiently. Processes like handing over rover operations from one facility to another, and continuing on a planned activity or procedure, should be practiced thoroughly beforehand.

3.3. Data processing and presentation

3.3.1. Issue/observation

It was not possible to completely define data visualization requirements before acquiring realistic data in the field setting. One example: Due to Poisson statistics inherent in the NSS measurement process, spatial smoothing was needed in the raster map visualization to highlight real trends in the data. Realistic NSS data from the rover was needed to determine the best type and amount of smoothing for the visualization.

3.3.2. Resolution

The ground data system software was built using very flexible high-level languages and libraries, and developers were on hand during the field testing. As new data visualization requirements were discovered early in the test, many could be satisfied with new features developed and used before the end of the test. This capability was vital to the success of the test. However, rapid software changes with minimal testing sometimes caused service outages in the ground data system that would be unacceptable in a real mission.

3.3.3. Recommendation

Projects should anticipate that visualization requirements will change during operations. In addition to prebuilt console displays that update in real-time, the ground data system should support an interactive plotting capability to enable more flexible data analysis, acting as a rapid prototyping sandbox for new console displays, and supporting the strategic planning process. In addition, proper modular software design and component isolation should be used, such that new experimental console displays can be added without impacting the stability of the rest of the ground data system.

4. Conclusions

The 2012 Hawai'i field exercise was extremely useful in demonstrating and improving a number of real-time operational procedures and tools. In terms of the ability to provide decision support, the test demonstrated the effectiveness of real-time monitoring of prospecting data. Clearly, efficiencies were gained from establishing clear thresholds in the data that trigger a transition from one mode of operation (*prospecting*) to another (*AIM* and subsequent decisions to auger, core or just carry on per the traverse plan). This is only possible in a mission with near real-time communications with Earth, and small delays, unlike Mars rover missions. Quick responses of this kind with manual intervention are practical only for missions with low-latency communications (Moon, NEO). For longer latencies (Mars, Outer Solar System), quick response requires onboard adaptive science capabilities, with a different set of technical and operational issues (Pedersen, 2001; Smith et al., 2007).

The scorecard for successful detection of potential resource targets is shown in Table 1, a list of the pre-emplaced targets and the results from the field exercise as executed. A total of 15 high-density polyethylene targets were emplaced. Four were never visited because the traverse plans were truncated or revised. Of the remaining 11, two were missed completely because of large deviations from the planned traverse path, partly related to telemetry issues and partly to mistaken hazard avoidance tele-operations from ExDOC. One target (Target 03) was missed due to a payload telemetry drop out; no NSS data were being received while the rover crossed the target. Another, Target 06, was initially missed due to avoidance deviations but was recovered by backtracking along the planned traverse path. Of the 9 targets that the rover actually crossed, all were detected, and 7 were mapped with an *AIM* procedure and characterized.

The RESOLVE Hawai'i 2012 campaign demonstrated the utility of neutron spectroscopy as a prospecting approach aboard a planetary rover. The hydrogen abundances as gauged by NSS data were consistent with the target designs that the out-of-simulation team members emplaced.

Acknowledgments

The authors thank Jerry Sanders, Bill Larson, and Jackie Quinn for their management of the July 2012 Hawai'i ISRU field campaign. We thank Katie Rogers for her role in organizing the mission operations and serving as the Flight Director during the analog mission. Greg Mattes served exceptionally as our Science console, and Jen Clevenger was our excellent timeline taskmaster. We thank RESOLVE lead systems engineer Jim Smith for outstanding contributions to the field campaign. We acknowledge the Canadian Space Agency (CSA) and Neptec for their contribution of the rover to this project, and PISCES (Pacific International Space Center for Exploration Systems) for their help in organizing the Hawai'i field test. The Human Exploration and Operations Mission Directorate/Advanced Exploration Systems made this test possible.

References

Colaprete, A., Schultz, P., Heldmann, J.L., Shirley, M., Ennico, K., Hermalyn, B., Wooden, D., Marshall, W., Ricco, A., Elphic, R.C., Goldstein, D., Summy, D., Bart, G., Asphaug, E., Korycansky, D., Lis, D., Sollitt, L., 2010. Detection of water in the LCROSS ejecta plume. Science 330, 463–468. http://dx.doi.org/10.1126/science.1186986.

Cristello, N., Faragalli, M., Jones, B. et al., 2013. The Lunar Analog ISRU Rover "Artemis Jr.", (abstract: http://robotics.estec.esa.int/ASTRA/Astra2013/Papers), 12th Symposium on Advanced Space Technologies in Robotics and Automation, 15–17 May 2013, Noordwijk, Netherlands.

Deans, M.C., Smith, T., Lees, D.S., Scharff, E.B., Cohen, T.E., 2013. Real time science decision support tools: development and field testing. In: 44th Lunar and Planetary Science Conference, LPI Contribution No. 1719, p.2847.

Elphic, R.C., Chu, P., Hahn, S., James, M.R., Lawrence, D.J., Prettyman, T.H., Johnson, J.B., Podgorney, R.K., 2008. Surface and downhole prospecting tools for planetary exploration: tests of neutron and gamma ray probes. Astrobiology 8 (3), 639–652. http://dx.doi.org/10.1089/ast.2007.0163.

Feldman, W.C., Maurice, S., Binder, A.B., Barraclough, B.L., Elphic, R.C., Lawrence, D.J., 1998. Fluxes of fast and epithermal neutrons from lunar prospector: evidence for water ice at the lunar poles. Science 281, 1496. http://dx.doi.org/10.1126/science.281.5382.1496.

Feldman, W.C., Barraclough, B.L., Fuller, K.R., Lawrence, D.J., Maurice, S., Miller, M.C., Prettyman, T.H., Binder, A.B., 1999. The lunar prospector gamma-ray and neutron spectrometers. Nucl. Instrum. Methods Phys. Res. A 422, 562–566. http://dx.doi.org/10.1016/S0168-9002(98)00934-6.

Feldman, W.C., Lawrence, D.J., Elphic, R.C., Barraclough, B.L., Maurice, S., Genetay, I., Binder, A.B., 2000. Polar hydrogen deposits on the Moon. J. Geophys. Res. Planets 105, 4175–4195. http://dx.doi.org/10.1029/1999JE001129.

Feldman, W.C., Boynton, W.V., Tokar, R.L., et al., 2002. Global distribution of neutrons from mars: results from mars odyssey. Science 297 (5578), 75–78. http://dx.doi.org/10.1126/science.1073541.

Gladstone, G.R., Retherford, K.D., Egan, A.F., et al., 2012. Far-ultraviolet reflectance properties of the Moon's permanently shadowed regions. J. Geophys. Res. 117, E00H04. http://dx.doi.org/10.1029/2011JE003913.

Goldsten, J.O., Rhodes, E.A., Boynton, W.V., Feldman, W.C., Lawrence, D.J., et al., 2007. The MESSENGER gamma-ray and neutron spectrometer. Space Sci. Rev. 131, 339–391. http://dx.doi.org/10.1007/s11214-007-9262-7.

Heldmann, J.L., Colaprete, A., Elphic, R.C., et al., 2015. Real-time science operations to support a lunar polar volatiles rover mission. Adv. Space Res. 55, 2427–2437.

Hurley, D.M., Lawrence, D.J., Bussey, D.B.J., Vondrak, R.R., Elphic, R.C., Gladstone, G.R., 2012. Two-dimensional distribution of volatiles in the lunar regolith from space weathering simulations. Geophys. Res. Lett. 39, L09203. http://dx.doi.org/10.1029/2012GL051105.

Mitrofanov, I.G., Bartels, A., Bobrovnitsky, Y.I., et al., 2010. Lunar exploration neutron detector for the NASA lunar reconnaissance orbiter. Space Sci. Rev. 150 (1–4), 183–207. http://dx.doi.org/10.1007/s11214-009-9608-4.

Paige, D.A., Siegler, M.A., Zhang, J.A., et al., 2010. Diviner lunar radiometer observations of cold traps in the moon's South Polar Region. Science 22, 479–482. http://dx.doi.org/10.1126/science.1187726.

Pedersen, L., 2001. Autonomous characterization of unknown environments. In: Proceedings of IEEE International Conference on Robotics and Automation (ICRA), pp. 277–284. http://dx.doi.org/10.1109/ROBOT.2001.932566.

Prettyman, T.H., Feldman, W.C., McSween, H.Y., et al., 2011. Dawn's gamma ray and neutron detector. Space Sci. Rev. 164, 371–459. http://dx.doi.org/10.1007/s11214-011-9862-0.

Roush, T.L., Colaprete, A., Elphic, R.C., et al., 2015. In Situ Resource Utilization (ISRU) field expedition 2012: Near-Infrared Volatile Spectrometer System (NIRVSS) science measurements compared to site knowledge. Adv. Space Res. 55, 2451–2456.

Sanders, G.B., Larson, W.E., 2015. Final review of analog field campaigns for In Situ Resource Utilization technology and capability maturation. Adv. Space Res. 55, 2381–2404.

Smith, T., Thompson, D.R., Wettergreen, D.S., Cabrol, N.A., Warren-Rhodes, K.A., Weinstein, S.J., 2007. Life in the Atacama: science autonomy for improving data quality. J. Geophys. Res. 112, G04S03. http://dx.doi.org/10.1029/2006JG000315.